

# Investigation of the Effect of Normal Incidence of RF Wave on Human Head Tissues Employing Cu and Ni Grid PET Films

Sai Spandana Pudipeddi  
Department of EECE  
School of Technology  
GITAM Deemed to be University  
Visakhapatnam, India  
psspandana26@gmail.com

Pappu V. Y. Jayasree  
Department of EECE  
School of Technology  
GITAM Deemed to be University  
Visakhapatnam, India  
jpappu@gitam.edu

Received: 11 August 2022 | Revised: 27 August 2022 | Accepted: 29 August 2022

**Abstract-**The rising number of frequency bands and the demand for wireless communication devices has become a growing concern regarding health and safety. The human head is a vulnerable body part when exposed to mobile phones. To ensure a high level of protection of the head from undesirable Electromagnetic Field (EMF) emissions, a shield is incorporated in this paper between the head and the mobile smartphone. The shielding material used to protect the head from the RF emissions is Copper (Cu) grid transparent Polyethylene Terephthalate (PET) film and Copper (Cu) grid transparent PET film with Nickel (Ni) coating forming a laminated mesh. The RF emission metric from the smartphone is determined to evaluate the Specific Absorption Rate (SAR) numerically with a variation in frequencies ranging from 850MHz to 5.47GHz at normal wave incidence by the Transmission Line Method. The variation in frequency is observed in two head models, one of an adult and one of a child. Compared with the no shield condition, a significant SAR reduction is observed when PET-Cu or PET-Cu-Ni conductive coating transparent shielded mesh is embodied on the front part of the mobile phone between the phone and the head. In the child 7-layered head model at 5.47GHz, a significant reduction in SAR is observed from 10.5W/kg to 0.00001W/kg using the Cu grid PET film and to 0.0000032W/kg using Cu and Ni grid PET film.

**Keywords-**RF radiation emissions; Specific Absorption Rate (SAR); shielding effectiveness; copper grid PET film; conductive coating

## I. INTRODUCTION

Many researchers have recently proposed altogether new designs of 5G antennas for cellular or wireless application to mitigate the effect of RF absorption emitted from mobile handsets [1-3]. The wireless communication devices emit most of the Electromagnetic Fields (EMFs) from unwanted electromagnetic interference [4]. A proper Electromagnetic Compatibility (EMC) technique is the need of the hour to mitigate such undesirable emissions from the devices, such as mobile smartphones [5]. Though many regulatory bodies

specify the Specific Absorption Rate (SAR) permissible limits, as and when the devices migrate to 5G frequency bands and higher and the radiation emission from the devices surges [6]. The EMFs and radiation spectrum consist of an extensive range of frequencies covering non-ionizing and ionizing radiation [4]. The non-ionizing radiation results in thermal and non-thermal effects on human bodies. The thermal effects are caused due to heating of the body due to a temperature rise in the tissues. The National Radiological Protection Board (NRPB) discussed the possibility of reducing the body SAR limit over 10g of tissue from averaged 10W/kg to 5W/kg, because the data indicated that the temperature rise in the eye and brain may exceed 1°C [7]. There is a fear of biological hazards occurring with the rise of temperature in the biological tissues of the brain of humans.

In order to protect the human head from the non-ionizing radiation of mobile smartphones, a shield can be incorporated between the human head and the mobile phone on the front side. The property of Shielding Effectiveness (SE) for a single or a laminated shield can be determined as a metric to measure the performance of any shielding material used. Many shielding materials have been used in the past to shield EM waves, such as polymer-based composites that include polymer matrixes and structured polymer composites, foams and aerogels, textile-based shielding materials, graphene, CNT-based or nanocomposites-based materials, etc. Due to various disadvantages and fitting the material for a particular scientific application, the researchers are now shifting their focus to transparent shielding material [4-5].

Most materials and their blends have been used in shielding the EM wave in various applications such as aerospace, electrical and electronic equipment, medical electronics, and wireless networks and devices. A very limited literature is available for the SAR measurement and distributions studies and implementation using shielding for mobile phone applications. Even with the implementation of SAR distribution, mobile phone emissions have been reduced using the usual electromagnetic software simulations [8-9]. Most of

the relative published studies have considered a modification in the mobile antenna design for their theoretical or experimental validation of SAR reduction.

Authors in [10] fabricated a transparent conductive electrode made of metal mesh film composed of Nickel mesh embedded on PET substrate achieving optical transparency of 84%. The Ni mesh was embedded with polymer poly (3,4-ethylenedioxythiophene): poly (styrenesulfonate) (PEDOT: PSS) for supercapacitor application [10]. Galvanic deposition of Cu-Ag and Ni-Ag on Ag seed mesh was obtained in X-band and K-band respectively. The SE increased from 23.2 to 43.7dB with 82.2% transparency, while 47.6dB SE was achieved for Cu-Ag mesh and Ni-Ag mesh respectively for electronic devices [11]. A Cu mesh with PET sheet as substrate was fabricated with visible transmittance of 85% in [12]. The shielding efficiency was tested in the range 12-18GHz and was 41dB. Indium Tin Oxide (ITO) layer was doped on PET substrate with 83.5% transparency for flexible electronics in [13]. The Cu/Ni/PEDOT: PSS Transparent Conducting Film (TCF) was fabricated with a transmittance of 86% for Joule heating purposes in [14].

A transparent shielded mesh film is employed as a shield in the current study, considering the disadvantages of several shielding materials. The primary properties of transparent materials are light weight, non-corrosiveness, flexibility, and durability for applications in electronics. An alternative to Transparent Conducting Oxides (TCO) is Transparent Conductive Coatings exhibiting the non-variant nature of electrical properties under flexing. Optical transparency is a crucial feature of transparent materials, which is inversely proportional to SE. SE of more than 60dB can be achieved with transparent shielded mesh film [15].

The novelty of the proposed work is the theoretical mitigation of the SAR absorbed in two head models of different ages from mobile smartphones operating at various bands from (850 to 5470MHz). Moreover, the SAR is minimized with the aid of SE of the laminated shielded mesh film by Transmission Line Method at the worst-case normal incidence of EM RF wave. The shielding material is transparent PET film with conductive Cu and Ni coatings forming a laminated mesh film.

II. MATERIALS AND METHODS

A. Transparent Conductive Metal Mesh PET Film

The transparent material used for the mathematical analysis is PET film with copper and nickel mesh conductive coatings. The structure constitutes a laminated shielded mesh. It is essential to derive shield and conductive mesh impedance and propagation constant in terms of conductivity, permeability, and permittivity [16]. Equations (1) and (2) give the PET film's shield impedance.

$$\eta = (1 + j) \sqrt{\frac{\pi f \mu}{\sigma}} \quad (1)$$

$$\gamma = \sqrt{j\omega\mu(\sigma + j\omega\epsilon)} \quad (2)$$

$$R_m = \frac{1}{\sigma\delta \left(1 - e^{-\frac{l_m}{\delta}}\right)} \left(\frac{g}{2a}\right) \quad (3)$$

$$X_m = z_0 \left(-\frac{g}{\lambda}\right) \left[ \ln \left( \sin \left( \frac{a\pi}{g} \right) \right) \right] \quad (4)$$

$$Z_m = \frac{1}{\eta_0} (R_m + jX_m) \quad (5)$$

where  $R_m$  and  $X_m$  are the resistance and reactance respectively of the Cu and Ni conductive coating.  $\delta$  is the skin depth,  $g$  and  $2a$  are mesh spacing and line-width, and  $l_m$  is the mesh thickness which is 100 and 50nm for Cu and Ni coating respectively [17]. The impedance  $Z_m$  of conductive mesh coatings is, thus, given by (5).

B. Head Models with Tissues

The head height of the adult and child head models is 25 and 23.5cm with diameters of 16.01 and 14.06cm respectively [18-20]. Multi-layered head models are considered in the current research. Head models with 4 and 7 layers of tissues are taken for analysis. Skin, fat, bone, and brain are the layers considered in the 4-layered model, whereas skin, fat, bone, dura, CSF, gray matter, and white matter are the tissue layers considered in the 7-layered model [21]. Their representation is shown in Figures 1 and 2. The analysis using the Transmission Line Method considers the spherical models to be planar (4 and 7 layers) as in Figures 3 and 4. The tissue thickness of the head is given in Tables I and II.

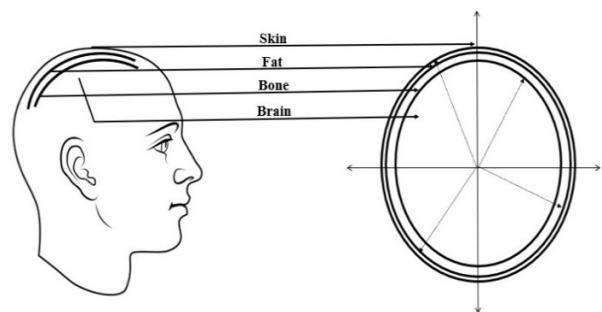


Fig. 1. Four-layered adult or child head model (Table I).

TABLE I. TISSUE THICKNESS OF 4 LAYERS IN ADULT AND CHILD HEAD MODELS [19-20]

Model	Tissue layer	Thickness (mm)
Adult	Skin	1
	Fat	2
	Bone	7
	Brain	70.05
Child	Skin	1
	Fat	0.5
	Bone	6.5
	Brain	62.3

C. SE Derivation

The reflection and transmission coefficients are derived from tissue medium's thickness, impedances, and propagation constants [22]. The conductivity and relative permittivity of each tissue medium is obtained from [23].

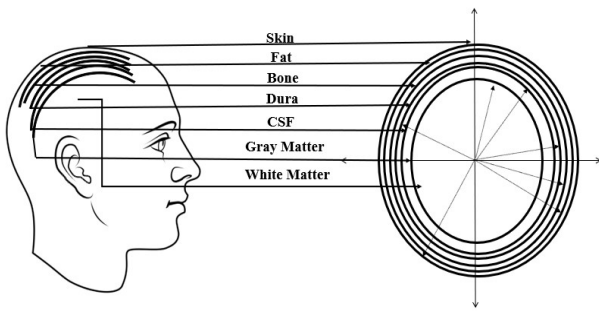


Fig. 2. Seven-layered adult or child head model (Table II).

TABLE II. TISSUE THICKNESS OF 7 LAYERS IN ADULT AND CHILD HEAD MODELS [21]

Model	Tissue layer	Thickness (mm)
Adult	Skin	1
	Fat	2
	Bone	7
	Dura	1.5
	CSF	2
	Gray Matter	3.7
	White Matter	62.85
Child	Skin	1
	Fat	0.5
	Bone	6.5
	Dura	0.5
	CSF	1.5
	Gray Matter	3.6
	White Matter	56.7

Also, the total transmission coefficient for the radiated EM wave is derived for the head model alone and then with the copper and nickel grid PET film (PET film with Cu mesh, and PET film with Cu, Ni mesh) from (6), (7), and (8).

$$T = p \prod_{k=Skin}^{Gray\ Matter} [(1 - q_{<k>} e^{-2\gamma_{<k>} l_{<k>}})] e^{-\gamma_{<k>} l_{<k>}} \quad (6)$$

$$T = p \prod_{k=PET+Cu}^{Gray\ Matter} [(1 - q_{<k>} e^{-2\gamma_{<k>} l_{<k>}})] e^{-\gamma_{<k>} l_{<k>}} \quad (7)$$

$$T = p \prod_{k=PET+Cu+Ni}^{Gray\ Matter} [(1 - q_{<k>} e^{-2\gamma_{<k>} l_{<k>}})] e^{-\gamma_{<k>} l_{<k>}} \quad (8)$$

where  $p$  represents the transmission coefficient, which is the product of the intrinsic impedances across the media and  $q$  represents the reflection coefficient, calculating the impedances across two consecutive interfaces.

#### D. SAR Computation from the SE of Head Models

Equation (6) represents the total transmission coefficient  $T$  of the radiated electromagnetic wave, considering the power entered into the skin through the layers of fat, bone, dura, CSF, and gray matter and propagated into the white matter. Equation (7) represents  $T$  of the radiated electromagnetic wave, considering the power entering into the Cu grid PET film through the intermediate tissue layers and gray matter respectively. The total radiated power into the white matter goes through the layers of Cu and Ni grid PET laminated shielded mesh film, skin, fat, bone, dura, CSF, and gray matter. The SE (dB) is evaluated from  $T$  as in (9) [24]. The  $E_i$  is computed from the incident wave power density delegated by the ICNIRP standard for mobile phone frequencies [25].  $E_t$  is obtained from the SE of the head without and with the laminated shielded mesh from (10).

$$SE = -20 \log_{10}|T| \quad (9)$$

$$SE = 20 \log_{10} \left( \frac{E_i}{E_t} \right) \quad (10)$$

The SAR is computed from the SE of the human head models (adult and child). By the ICNIRP guidelines, the power densities of the incident wave at frequencies of 5.47, 4.5, 3.6, and 2.3GHz, are  $40W/m^2$ ,  $36.556W/m^2$  at 1.8GHz and  $19.175W/m^2$  at 0.85 GHz [25]. The SAR absorbed (W/kg) by  $i$  (brain/white matter) in a (4/7-layered head model) of an adult and child is given by:

$$SAR = \frac{\sigma_i E_t^2}{\rho_i} \quad (11)$$

The allowable SAR limit proposed by ICNIRP is 2W/kg for absorption by local body parts such as head/limbs.

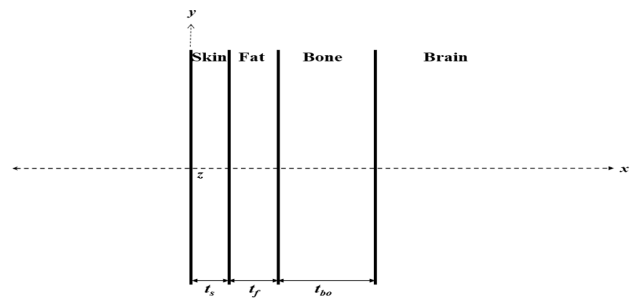


Fig. 3. Four-layered planar head model with the adult/child tissue thickness.

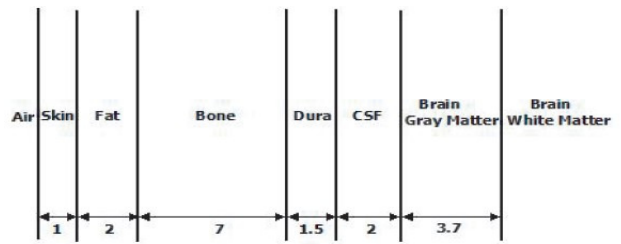


Fig. 4. Seven-layered planar head model with the adult head tissue thickness [23]. Reproduced, courtesy of The Electromagnetics Academy.

### III. RESULTS AND DISCUSSION

The SE plots of 4- and 7-layered head models of adult and child for frequencies ranging from 850 to 5470MHz without shield, with transparent conductive metal (Cu and Ni), and with mesh PET film for normal incidence of EM wave is shown in Figures 5 and 6 and Figures 7 and 8 respectively.

The wave's frequency in any medium is directly proportional to the medium's SE. The SE against the frequency of the head model in the child is less than that of the adult head model in Figures 5-8. The SE of a child's 7-layered head model from Figure 8 is only around 20dB without the laminated shield and around 100dB with the copper grip PET film with Ni coating. Coincidence in graphs of the SE with frequency variation is noticed in the Figures because the thickness difference between Cu and Ni metal mesh coatings is only 50nm. The SAR emission absorbed by the brain in the 4-layered adult and child head models is tabulated in Tables III

and IV. At 5.47GHz frequency, the Cu grid PET Film with Ni coating has absorbed a SAR of 5.91e-7W/kg in the adult 4-layered model and the child head model absorbed a comparatively higher SAR of 0.00002W/kg. Regarding the 7-layered model, the SAR absorbed by the white matter in the adult head model is 5.27e-09W/kg, which is less compared to that of the child's head model, which is 3.16e-06W/kg at 5.47GHz.

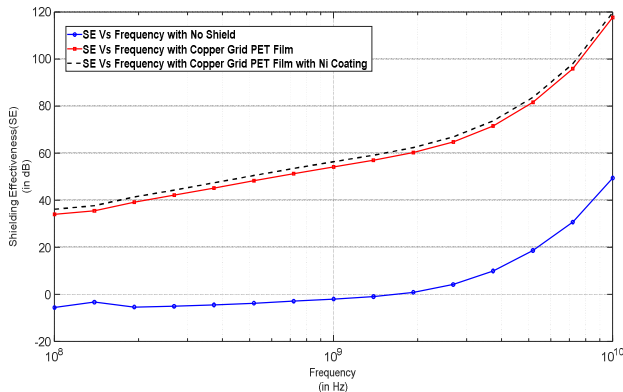


Fig. 5. SE with frequency variation of an adult 4-layered head model for no shield condition, with transparent Cu PET mesh film, and transparent Cu and Ni PET mesh film for normal incidence of EM wave.

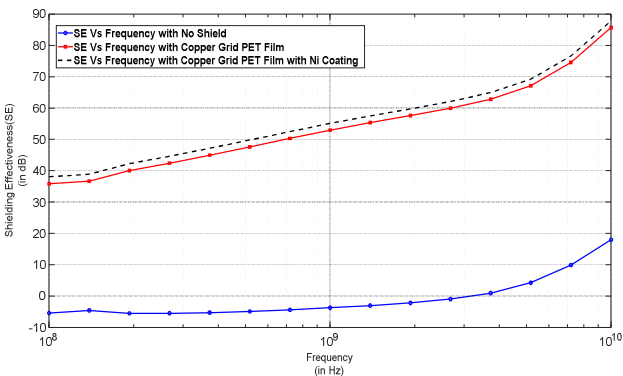


Fig. 6. SE with frequency variation of a child 4-layered head model for no shield condition, with transparent Cu PET mesh film, and transparent Cu and Ni PET mesh film for normal incidence of EM wave.

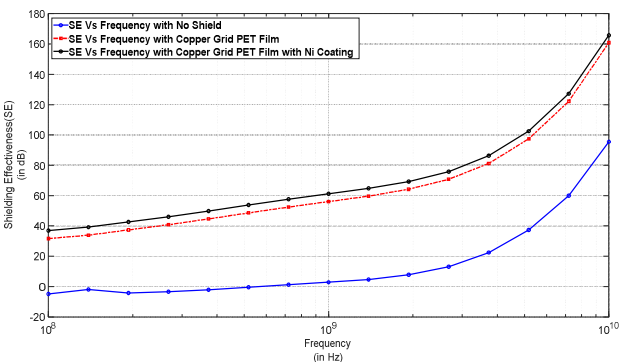


Fig. 7. SE with frequency variation of an adult 7-layered head model for no shield condition, with transparent Cu PET mesh film, and transparent Cu and Ni PET mesh film for normal incidence of EM wave.

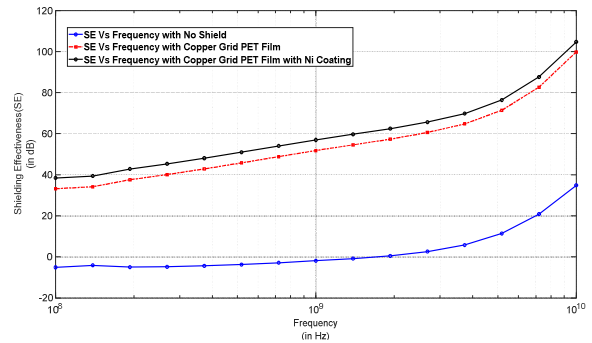


Fig. 8. SE with frequency variation of a child 7-layered head model for no shield condition, with transparent Cu PET mesh film, and transparent Cu and Ni PET mesh film for normal incidence of EM wave.

TABLE III. BRAIN SAR OF THE ADULT 4-LAYERED MODEL

Frequency GHz	SAR (W/kg)		
	Without shield	With Cu Grid PET film	With Cu Grid PET Film with Ni coating
0.85	31.8	9.47E-05	5.74E-05
1.8	49.11	6.08E-05	3.71E-05
2.3	42.14	4.19E-05	2.56E-05
3.6	14.77	1.03E-05	6.34E-06
4.5	5.82	3.37E-06	2.07E-06
5.47	2.05	9.58E-07	5.91E-07

TABLE IV. BRAIN SAR OF THE CHILD 4-LAYERED MODEL

Frequency GHz	SAR (W/kg)		
	Without shield	With Cu Grid PET film	With Cu Grid PET Film with Ni coating
0.85	43.34	1.6e-4	7e-5
1.8	90.55	1e-4	6.16e-5
2.3	103.12	9.29e-5	5.68e-5
3.6	100.52	6.62e-5	4.07e-5
4.5	87.57	5e-5	3.07e-5
5.47	66.83	3.25e-5	2e-5

TABLE V. WHITE MATTER SAR OF THE ADULT 7-LAYERED MODEL

Frequency GHz	SAR (W/kg)		
	Without shield	With Cu Grid PET film	With Cu Grid PET Film with Ni coating
0.85	9.84	5.84E-05	1.77E-05
1.8	9.32	2.29E-05	7.04E-06
2.3	6.1	1.20E-05	3.70E-06
3.6	0.33	4.49E-07	1.40E-07
4.5	0.15	1.63E-07	5.14E-08
5.47	0.02	1.67E-08	5.27E-09

TABLE VI. WHITE MATTER SAR OF THE CHILD 7-LAYERED MODEL

Frequency GHz	SAR (W/kg)		
	Without shield	With Cu Grid PET film	With Cu Grid PET Film with Ni coating
0.85	24.51	1.3e-4	3.97E-05
1.8	43.77	9.67E-05	2.97E-05
2.3	44.73	7.96E-05	2.46E-05
3.6	20.86	2.70E-05	8.43E-06
4.5	20.08	2.24E-05	7.03E-06
5.47	10.55	1.00E-05	3.16E-06

## IV. CONCLUSION

A theoretical investigation for the determination of the Specific Absorption Rate (SAR) of age-dependent multi-layered head models exposed to RF emissions from mobile phone operating frequencies of 850MHz-5.47 GHz for normal incidence of EM wave is assessed in this paper. Absorption is found with the relevance of shielding effectiveness of the human head in the absence of any shield and in the presence of Cu grid PET film (transparent conductive metal mesh PET film/transparent Cu PET laminated mesh) and Cu grid PET film with Ni coating. The result analysis at 5.47GHz showed that the child head model had absorbed a higher radiation level of 66.83W/kg in the 4-layered model and 10.55W/kg in the 7-layered model. The same model with the transparent PET and Cu laminated shielded mesh had absorbed a SAR of 0.0000325W/kg (4-layered model) and 0.00001W/kg (7-layered model). With the PET/Cu/Ni laminated mesh, 0.00002W/kg was absorbed by brain tissue by the 4-layered model, and white matter absorbed 0.00000316W/kg in the 7-layered head model of a child. Thus, a higher amount of SAR is reduced in adult head models compared to child head models using the transparent Cu grid PET film with Ni coating. Without a shield, the child model had absorbed maximum radiation of around 67W/kg and the PET laminated mesh film absorbed a comparatively negligible amount of SAR in every case.

## REFERENCES

- [1] D. T. T. My, H. N. B. Phuong, T. T. Huong, and B. T. M. Tu, "Design of a Four-Element Array Antenna for 5G Cellular Wireless Networks," *Engineering, Technology & Applied Science Research*, vol. 10, no. 5, pp. 6259–6263, Oct. 2020, <https://doi.org/10.48084/etasr.3771>.
- [2] S. Ghnimi, A. Nasri, and A. Gharsallah, "Study of a New Design of the Planar Inverted-F Antenna for Mobile Phone Handset Applications," *Engineering, Technology & Applied Science Research*, vol. 10, no. 1, pp. 5270–5275, Feb. 2020, <https://doi.org/10.48084/etasr.3287>.
- [3] B. P. Nadh, B. T. P. Madhav, and M. S. Kumar, "Design and analysis of dual band implantable DGS antenna for medical applications," *Sādhanā*, vol. 44, no. 6, May 2019, Art. no. 131, <https://doi.org/10.1007/s12046-019-1099-8>.
- [4] H. Aniolczyk, "EM Noise and Its Impact on Human Health and Safety," in *Advanced Materials for Electromagnetic Shielding*, M. Jaroszewski, S. Thomas, and A. V. Rane, Eds. John Wiley & Sons, Ltd, 2018, pp. 11–33, <https://doi.org/10.1002/9781119128625.ch2>.
- [5] R. Kitchen, *RF and Microwave Radiation Safety*, 2nd ed. Boston, USA: Newnes, 2001.
- [6] J. S. Seybold, *Introduction to RF Propagation*. Hoboken, NJ, USA: Wiley-Interscience, 2005.
- [7] "IEEE Standard for Safety Levels with Respect to Human Exposure to Radio Frequency Electromagnetic Fields, 3 kHz to 300 GHz," *1999 Edition IEEE Std C95*, Apr. 1999, <https://doi.org/10.1109/IEEESTD.1999.89423>.
- [8] T. B. Rashid and H. H. Song, "Analysis of biological effects of cell phone radiation on human body using specific absorption rate and thermoregulatory response," *Microwave and Optical Technology Letters*, vol. 61, no. 6, pp. 1482–1490, 2019, <https://doi.org/10.1002/mop.31777>.
- [9] A. M. Tamim, M. R. I. Faruque, M. U. Khandaker, M. T. Islam, and D. A. Bradley, "Electromagnetic radiation reduction using novel metamaterial for cellular applications," *Radiation Physics and Chemistry*, vol. 178, Jan. 2021, Art. no. 108976, <https://doi.org/10.1016/j.radphyschem.2020.108976>.
- [10] Y.-H. Liu, J.-L. Xu, S. Shen, X.-L. Cai, L.-S. Chen, and S.-D. Wang, "High-performance, ultra-flexible and transparent embedded metallic mesh electrodes by selective electrodeposition for all-solid-state supercapacitor applications," *Journal of Materials Chemistry A*, vol. 5, no. 19, pp. 9032–9041, May 2017, <https://doi.org/10.1039/C7TA01947E>.
- [11] A. S. Voronin *et al.*, "Cu–Ag and Ni–Ag meshes based on cracked template as efficient transparent electromagnetic shielding coating with excellent mechanical performance," *Journal of Materials Science*, vol. 56, no. 26, pp. 14741–14762, Sep. 2021, <https://doi.org/10.1007/s10853-021-06206-4>.
- [12] S. Walia, A. K. Singh, V. S. G. Rao, S. Bose, and G. U. Kulkarni, "Metal mesh-based transparent electrodes as high-performance EMI shields," *Bulletin of Materials Science*, vol. 43, no. 1, Aug. 2020, Art. no. 187, <https://doi.org/10.1007/s12034-020-02159-7>.
- [13] W. Zhou *et al.*, "Copper Mesh Templated by Breath-Figure Polymer Films as Flexible Transparent Electrodes for Organic Photovoltaic Devices," *ACS Applied Materials & Interfaces*, vol. 8, no. 17, pp. 11122–11127, May 2016, <https://doi.org/10.1021/acsami.6b01117>.
- [14] L. Zhao, S. Yu, J. Li, M. Wu, L. Li, and X. Wang, "Highly reliable flexible transparent conductors prepared with Cu/Ni grid by vacuum-free solution process," *Optical Materials*, vol. 120, Oct. 2021, Art. no. 111427, <https://doi.org/10.1016/j.optmat.2021.111427>.
- [15] B. Ray, S. Parmar, and S. Datar, "Flexible and Transparent EMI Shielding Materials," in *Advanced Materials for Electromagnetic Shielding*, M. Jaroszewski, S. Thomas, and A. V. Rane, Eds. John Wiley & Sons, Ltd, 2018, pp. 167–175, <https://doi.org/10.1002/9781119128625.ch8>.
- [16] R. B. Schulz, V. C. Plantz, and D. R. Brush, "Shielding theory and practice," *IEEE Transactions on Electromagnetic Compatibility*, vol. 30, no. 3, pp. 187–201, Dec. 1988, <https://doi.org/10.1109/15.3297>.
- [17] Y. L. and J. Tan, "Frequency Dependent Model of Sheet Resistance and Effect Analysis on Shielding Effectiveness of Transparent Conductive Mesh Coatings," *Progress In Electromagnetics Research*, vol. 140, pp. 353–368, 2013, <https://doi.org/10.2528/PIER13050312>.
- [18] B. Rajagopal and L. Rajasekaran, "SAR assessment on three layered spherical human head model irradiated by mobile phone antenna," *Human-centric Computing and Information Sciences*, vol. 4, no. 1, Aug. 2014, Art. no. 10, <https://doi.org/10.1186/s13673-014-0010-1>.
- [19] A. Drossos, V. Santomaa, and N. Kuster, "The dependence of electromagnetic energy absorption upon human head tissue composition in the frequency range of 300-3000 MHz," *IEEE Transactions on Microwave Theory and Techniques*, vol. 48, no. 11, pp. 1988–1995, Aug. 2000, <https://doi.org/10.1109/22.884187>.
- [20] S. Hout and J.-Y. Chung, "Design and Characterization of a Miniaturized Implantable Antenna in a Seven-Layer Brain Phantom," *IEEE Access*, vol. 7, pp. 162062–162069, 2019, <https://doi.org/10.1109/ACCESS.2019.2951489>.
- [21] S. S. Pudipeddi, P. V. Y. Jayasree, and S. G. Chintala, "Polarization Effect Assessment of Sub-6 GHz Frequencies on Adult and Child Four-Layered Head Models," *Engineering, Technology & Applied Science Research*, vol. 12, no. 4, pp. 8954–8959, Aug. 2022, <https://doi.org/10.48084/etasr.5096>.
- [22] "Calculation of the Dielectric Properties of Body Tissues in the frequency range 10 Hz - 100 GHz," *IFAC*. <http://niremf.ifac.cnr.it/tissprop/htmlclie/htmlclie.php>.
- [23] S. S. Pudipeddi and P. V. Y. Jayasree, "Numerical Computation of SAR in Human Head with Transparent Shields Using Transmission Line Method," *Progress In Electromagnetics Research M*, vol. 105, pp. 31–44, 2021, <https://doi.org/10.2528/PIERM21080405>.
- [24] International Commission on Non-Ionizing Radiation Protection (ICNIRP), "Guidelines for Limiting Exposure to Electromagnetic Fields (100 kHz to 300 GHz)," *Health Physics*, vol. 118, no. 5, pp. 483–524, May 2020, <https://doi.org/10.1097/HP.0000000000001210>.